First Measurement of the Hadronic Final State Charge Asymmetry in High Q^2 Deep-Inelastic Scattering at HERA

Daniel Traynor[1] *

1- Queen Mary, University of London - Physics
Mile End Road, London E10 6LN - UK

A first measurement has been made of the charge asymmetry in the scattered hadronic final state from the hard interaction in high Q^2 ($100 < Q^2 < 8,000$ GeV^2) deep-inelastic ep neutral current scattering at HERA. The difference between the event normalised distribution of the scaled momentum, x_p, for positively and negatively charged particles, measured in the current region of the Breit frame, has been studied together with its evolution as a function of Q. The results are compared to Monte Carlo models at the hadron and parton level.

1 Introduction

This article summarises a talk given at the DIS2009 Workshop [1].

In lepton proton deep-inelastic scattering (DIS) at large Bjorken x the contribution of u valence quarks from the proton to the hard interaction dominates over that from the d valence quarks due to their larger charge and greater abundance. Hence an asymmetry in the number of positively and negatively charged particles is observed in the final state [2]. It has been demonstrated that the charge sign asymmetry of the hadronic final state in pp collisions at RHIC [3] is sensitive to the valence quark distribution [4].

In a recent paper, H1 presented a study of the inclusive charged particle production in high Q^2 deep-inelastic scattering (DIS) at HERA [5]. The measurement is performed in the current hemisphere of the Breit frame [6]. In the naïve quark parton model (QPM) the momentum of the scattered parton in the Breit frame is $Q/2$, where Q^2 is the virtuality of the exchanged boson. The main observable studied is x_p, the charged particle momentum in the current region of the Breit frame scaled to $Q/2$.

General agreement was observed between ep, ee data and Monte Carlo predictions, broadly supporting the concept of quark fragmentation universality. Hadrons with small values of x_p are predominately produced by fragmentation. While hadrons at large x_p are more likely to contain a parton from the hard interaction. Therefore a study of the x_p distribution separately for positively and negatively charged particles should reveal information about the valence quarks and their fragmentation.

2 Data Selection and Correction

A description of the H1 detector can be found elsewhere in [7]. The data used in this analysis correspond to an integrated luminosity of 44 pb^{-1} and were taken by H1 in the year 2000 when protons with an energy of 920 GeV collided with positrons with an energy of 27.5 GeV.

*On behalf of the H1 collaboration

Events are selected if the scattered positron is detected in the LAr calorimeter in the polar angular range $10^\circ < \theta_e < 150^\circ$ and with energy greater than 11 GeV. The kinematic phase space, calculated using the scattered positron only, is defined by requiring the negative squared photon momentum to be in the range $100 < Q^2 < 8\,000\text{GeV}^2$ and the inelasticity y_e, which is the fractional energy loss of the positron in the proton rest frame, to be in the range $0.05 < y_e < 0.6$. The polar scattering angle for a massless parton, calculated from the positron kinematics in the quark-parton model (QPM) approximation is required to be in the range $30^\circ < \theta_{q,lab} < 150^\circ$. This ensures that the current region of the Breit frame remains in the central region of the detector where there is high acceptance and track reconstruction efficiency. It should be noted that the kinematic phase space can be defined solely from the scattered electron and applied in a simple way to theoretical models.

Additional selections are made to reduce QED radiation effects and to suppress background events (photoproduction, beam gas and Compton QED). The final event selection results in a data sample of about 60,000 events.

The reconstructed charged tracks in the selected events are used to study the fragmentation process. Only tracks that are fitted to the primary vertex and have transverse momenta above 120 MeV are used in this analysis. In addition a variety of other track quality cuts (track length, number of hits on a track, the χ^2 of the track fit etc) are applied to remove badly measured tracks in a manner which can be accurately simulated. The contribution from the in-flight decays of K^0's, Λ's, and from photon conversions and other secondary decays is minimised by using only those tracks fitted to the event vertex.

The data are corrected for detector acceptance, efficiency, resolution effects, and QED radiation. The total correction factor applied to the uncorrected data points is typically $1.0 - 1.2$ for $D(x_p, Q)$. In the measurement of the charge asymmetry ratio contributions to the correction factor mostly cancel and as a result the correction factor is consistent with 1.0.

Several sources of systematic errors are considered, including; the scattered positron energy scale uncertainty and angular resolution, the hadronic energy scale uncertainty, the model uncertainty from the correction procedure, and the track reconstruction efficiency. All sources of error are treated as uncorrelated, apart from the positron energy scale uncertainty which is treated as fully correlated between bins. For $D(x_p)$ the largest contributions to the systematic error are the positron energy scale uncertainty, 0.5% ($x_p \sim 0.1$) to 11% ($x_p \sim 1.0$), and the track reconstruction uncertainty, 2.5%. For the charge asymmetry measurements the systematic errors mostly cancel and the only significant contribution is from the track reconstruction uncertainty, 2.5%.

3 Phenomenology

The data are compared to predictions of the Parton Shower model (PS) [8], as implemented in the RAPGAP [9] Monte Carlo program , and to predictions of the Colour Dipole Model (CDM) [10] both matched to $O(\alpha_s)$ matrix elements. ARIADNE [11] provides an implementation of CDM and is used in the DJANGO [12] Monte Carlo program. Both the PS and CDM predictions use the Lund string model for hadronisation [13]. The HERWIG Monte Carlo [14] program uses the parton shower model to describe the fragmentation process but incorporates the cluster model of hadronisation [15]. The data are also compared to predictions from the Soft Colour Interaction model (SCI) [16] using the generalised area law (GAL) [17] as implemented in LEPTO [18]

It is possible to turn off the hadronisation and compare data with parton level predictions using the assumption of local parton hadron duality. This has been done with the CDM predictions where a quark, with fractional charge, is taken as equivalent to a charged hadron of unit charge. The predictions are made after the main parton cascade has taken place and the gluons are ignored.

The CTEQ5L PDF [19] is used for all model predictions. However other PDFs lead to charge asymmetries in agreement with the prediction based on CTEQ5L to within $\pm$ 0.01.

4 Results

The scaled momentum distribution for all charged particles, and for positive, and negative particles separately, is shown in figure 1a). As seen in many previous publications, there are significantly more particles produced at low x_p than at high x_p. This is understood as follows. Partons are produced from the hard interaction with large values of x_p. By the process of fragmentation many more particles are produced with low values of x_p, while few particles are left at high x_p. However, the particles left at high x_p retain information of the partons produced in the hard interaction. Sea quarks and gluons will produce, on average, charged symmetric hadronic final states. As a result any charge asymmetry is expected to be caused by the different numbers, and couplings, of u and d valence quarks, and should still be visible at high x_p. The scaled momentum distribution for positive and negative particles are very similar at low x_p but at high x_p there is a clear excess of positive particles.

The charge asymmetry can be as large as 20% as shown in figure 1b). The scaled momentum distribution and its asymmetry is described by the Monte Carlo models. Models using string hadronisation (PS, CDM, GAL) produce a smaller charge asymmetry at high x_p than that produced by the cluster hadronisation model (HERWIG). Similar differences between the models at high x_p were observed in [5].

In figure 1c) the charge asymmetry is compared to predictions from CDM before and after hadronisation. It is observed that at high x_p the hadron and quark levels are in good agreement and both agree with the data. However, as x_p get smaller a large difference develops with the quark level asymmetry prediction which is constant at $\sim 12\%$, while the hadron level, and the data, fall to zero. This is consistent with the expectation that the hadrons at low x_p are dominantly produced by fragmentation while hadrons at high x_p retain the memory of the charge of the scattered quark from the hard interaction.

Figures 2 shows the charge asymmetry as a function of Q in different x_p intervals. The charge asymmetry clearly evolves to larger values as Q increases. The largest asymmetries of up to 40% are obtained in the highest Q and highest x_p intervals. It should be noted that higher average Q corresponds to higher average x and hence the highest Q intervals are most sensitive to the valence quark distribution. The distributions are well described by the Monte Carlo models.

5 Conclusions

The first measurement of the charge asymmetry of the hadronic final state at HERA is presented. The charge asymmetry is found to be dependent on the scaled momentum x_p with a larger asymmetry for larger x_p. The observed charge asymmetry at large x_p is found to increase with the scale Q corresponding at HERA to an enhancement at large Bjorken x. The results are consistent with the expectation that the asymmetry is directly related to

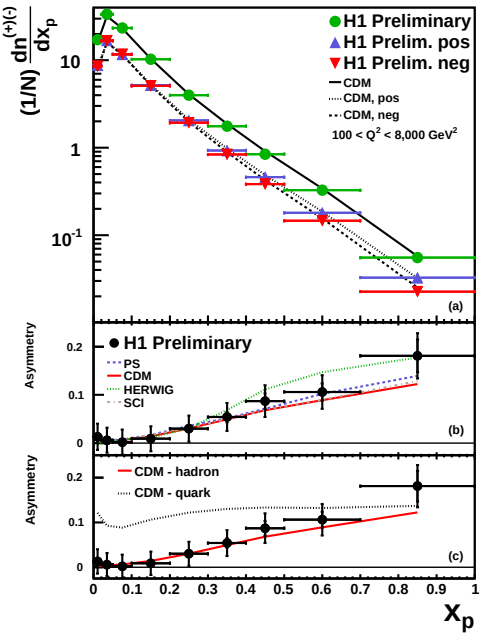

Figure 1: (a) The measured normalised distributions of the scaled momentum, $D(x_p)$, for all charged particles and for positively (pos) and negatively (neg) charged particles separately, and (b, c) the charge asymmetry, as a function of x_p. The error bars include statistical (inner), and statistical plus systematic errors added in quadrature (outer). The data are compared to predictions from different models of the parton cascade and hadronisation processes and to the parton level before hadronisation.

the valence quark content of the proton. The observed charge asymmetry is reproduced by various models. The data are expected to provide useful information for the extraction of fragmentation functions and additional constraints on the valence quark distribution of the proton.

References

[1] Slides:
`http://indico.cern.ch/contributionDisplay.py?contribId=289&sessionId=3&confId=53294`

[2] J. P. Albanese *et al.* [European Muon Collaboration], Phys. Lett. B **144** (1984) 302.
M. Arneodo *et al.* [European Muon Collaboration], Z. Phys. C **40** (1988) 347.

[3] J. Adams *et al.* [STAR Collaboration], Phys. Lett. B **637** (2006) 161, [nucl-ex/0601033];
I. Arsene *et al.* [BRAHMS Collaboration], Phys. Rev. Lett. **98** (2007) 252001, [hep-ex/0701041].

[4] S. Albino, B. A. Kniehl and G. Kramer, [hep-ph/0803.2768].

[5] F. D. Aaron *et al.* [H1 Collaboration], Phys. Lett. B **654** (2007) 148 [hep-ex/0706.2456].

[6] R. P. Feynman, Benjamin, N.Y. (1972).

[7] I. Abt *et al.* [H1 Collaboration], Nucl. Instrum. Meth. A **386** (1997) 310;
I. Abt *et al.* [H1 Collaboration], Nucl. Instrum. Meth. A **386** (1997) 348.

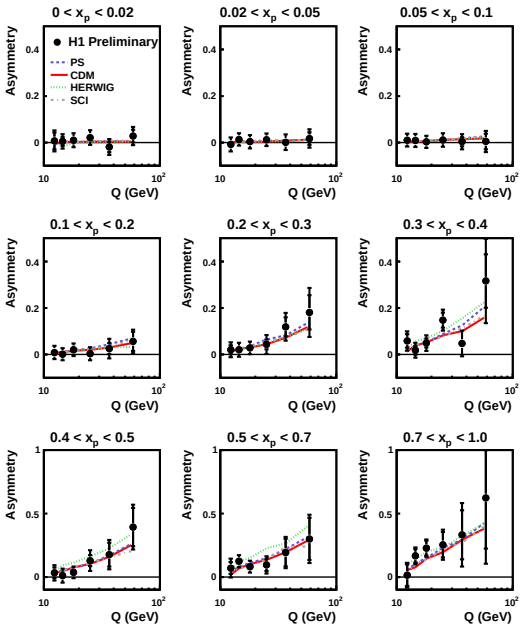

Figure 2: The charge asymmetry, as a function of Q for nine different x_p regions. The data are displayed at the average value of Q. The error bars include statistical (inner), and statistical plus systematic errors added in quadrature (outer). The data are compared to predictions from different models of the parton cascade and hadronisation processes.

[8] M. Bengtsson and T. Sjöstrand, Z. Phys. C **37** (1988) 465.

[9] H. Jung, Comput. Phys. Commun. **86** (1995) 147, RAPGAP version 3.1 is used.

[10] G. Gustafson, Phys. Lett. B **175** (1986) 453;
B. Andersson *et al.*, Z. Phys. C **43** (1989) 625.

[11] L. Lönnblad, Comput. Phys. Commun. **71** (1992) 15, ARIADNE version 4.12 is used.

[12] A. Kwiatkowski, H. Spiesberger and H. J. Mohring, Comput. Phys. Commun. **69** (1992) 155;
K. Charchula, G. A. Schuler and H. Spiesberger, Comput. Phys. Commun. **81** (1994) 381, DJANGOH version 1.4 is used.

[13] B. Andersson *et al.*, Phys. Rept. **97** (1983) 31.

[14] G. Marchesini *et al.*, Comput. Phys. Commun. **67** (1992) 465, HERWIG version 6.5 is used.

[15] B. R. Webber, Nucl. Phys. B **238** (1984) 492;
G. Marchesini and B. R. Webber, Nucl. Phys. B **310** (1988) 461.

[16] A. Edin, G. Ingelman and J. Rathsman, Phys. Lett. B **366** (1996) 371 [hep-ph/9508386], LEPTO version 6.5 is used.

[17] J. Rathsman, Phys. Lett. B **452** (1999) 364 [hep-ph/9812423].

[18] G. Ingelman, A. Edin and J. Rathsman, Comput. Phys. Commun. **101** (1997) 108 [hep-ph/9605286].

[19] H. L. Lai *et al.* [CTEQ Collaboration], Eur. Phys. J. C **12** (2000) 375 [hep-ph/9903282].